Tetrahedron 64 (2008) 5404–5409

Contents lists available at ScienceDirect

Tetrahedron

journal homepage: www.elsevier.com/locate/tet

Synthesis, electrochemical, and spectroscopic properties of soluble perylene monoimide diesters

Lanying Yang [a,b], Minmin Shi [a,b,*], Mang Wang [a,b], Hongzheng Chen [a,b,*]

[a] Department of Polymer Science and Engineering, State Key Lab of Silicon Materials, Zhejiang University, Hangzhou 310027, PR China
[b] Key Laboratory of Macromolecule Synthesis and Functionalization, Zhejiang University, Ministry of Education, Hangzhou 310027, PR China

ARTICLE INFO

Article history:
Received 17 September 2007
Received in revised form 26 February 2008
Accepted 29 February 2008
Available online 18 March 2008

ABSTRACT

Perylene derivatives are an important class of n-type semiconductors. With the exceptions of bay-substituted and *N*-swallow-tail alkyl/*tert*-butyl substituted derivatives, most perylene diimides are insoluble. The recently reported perylene tetraesters are highly soluble, but are less electron-deficient. In this paper, a series of perylene monoimide diesters have been synthesized, which have good solubility and acceptable electron-accepting property due to the introducing of imide and ester groups in one perylene molecule. Their electrochemical properties and structural ordering were examined by cyclovoltammetry and X-ray diffraction technique, respectively. Their absorption and emission spectra are reported and discussed.

1. Introduction

Optoelectronic devices based on organic semiconductors, such as organic field-effect transistors (OFETs),[1] light-emitting diodes (OLED),[2] solar cells,[3] sensors,[4] and organic memory devices,[5] have recently gained great attention due to their advantages over conventional inorganic devices, including low cost of fabrication, simple package, compatibility with flexible substrate, and immense variety of molecular semiconductors. In addition, the promise of eventually being able to synthetically optimize molecular materials for desired properties also motivates this work. n-Type organic semiconductors are key components of organic p–n junctions, bipolar transistors, and complementary integrated circuits, leading to flexible, large-area, and low cost electronic applications.[6] But compared with p-type organic semiconductors, such as pentacene,[7] oligothiophenes,[8] and phthalocyanines,[9] n-type semiconductors are not fully developed. To obtain high electron mobility, n-type organic semiconductors should be highly ordered with strong intermolecular interactions and should also have a proper LUMO energy level. In addition, soluble materials are more designed due to the superiority of solution-processing.

Perylene diimides are a particularly promising class of dyes for n-type semiconductors available to date.[10] However, they are generally insoluble and therefore have to be deposited by sublimation. To fully exploit the cost advantage associated with organic semiconductors, solution-processing such as spin- or dip-coating is preferred, which needs soluble perylene derivatives to be developed. In fact, soluble perylene diimides have been developed successfully either by introducing solubilizing *N*-substituents, e.g., long-chain secondary (swallow-tail) alkyl groups and *tert*-butyl groups,[11] or by introducing substituents at the carbocyclic scaffold (the so-called bay-area).[12] For example, Müllen designed ingeniously a series of perylene diimide-based dendrimers, making it possible to investigate thoroughly energy and electron transfer at single-molecule level;[13] Würthner built many functional supramolecular architectures through hydrogen bonding, metal ion coordination, and π–π stacking interactions with soluble perylene dimides as building blocks;[14] Tian also synthesized some new soluble perylene dyes, and explored their potential applications in solar cells, electron acceptors, luminescent materials, and light switches.[15] Unfortunately, the solubility of perylene diimide is gained at the expense of the coupling offset between adjacent perylene molecules as a result of the steric effect or the twisting of the perylene core.[11,16] It is believed that the coupling between chromophores is an important factor in realization of high-performance photoconductive devices.[17]

Recently, the tetraalkyl esters of perylene-3,4,9,10-tetracarboxylic acid (perylene tetraesters) were reported to be a potentially large new class of self-organizing electron transport materials.[18] They are highly soluble in common organic solvents resulted from the introduction of four flexible alkyl chains, and thus are solution-processible. Due to the weak intermolecular coupling as deduced from the similar absorption spectra in solid and solution,[18] films of perylene tetraesters exhibited weak emission quenching and thus have been successfully used as light-emitting layer in red OLEDs.[19] However, the device performance was poor when

---

[*] Corresponding authors. Tel.: +86 571 8795 2557; fax: +86 571 8795 3733.
E-mail addresses: minminshi@zju.edu.cn (M. Shi), hzchen@zju.edu.cn (H. Chen).

0040-4020/$ – see front matter © 2008 Elsevier Ltd. All rights reserved.
doi:10.1016/j.tet.2008.02.104

perylene tetraesters were used in solar cells due to the limit of dissociation of excitons,[20] which was the result of their less electron-deficient property compared with perylene diimides owing to the much less coplanarity with perylene core of the ester groups than imide groups.[21]

Considering the above demonstrations, we think that the combination of imide and ester groups in one molecule should result in good solubility and acceptable electron-accepting property simultaneously. In this paper, such a type of perylene derivatives, namely perylene monoimide diesters, were designed and synthesized for the first time through a simple phase-transfer catalysis reaction. The molecular structure, electrochemical properties, and the structural ordering were fully characterized. The absorption and emission spectra were recorded and were explained in detail by the exciton theory and film ordering, respectively.

2. Results and discussion

2.1. Synthesis

The target compounds studied in this paper were prepared via a two-step procedure outlined in Scheme 1. First, the monoimide **2** was synthesized by treating dianhydride **1** with ammonia in water and was separated from the diimide byproduct and the unreacted dianhydride **1** based on their different solubility in alkaline aqueous solution.[22] The further purified **2** via vacuum sublimation was then subjected to a phase-transfer catalysis reaction to produce the final product **3**.[23] By changing the length of the alkyl substituents from 4, 8 to 12 carbon atoms, **3** compounds abbreviated as **3a**–**c** were obtained. The target compounds were characterized with FTIR spectroscopy and ^{1}H NMR. The purity of the compounds was determined by elemental analysis, which was in good agreement with the calculated values, indicating that these perylene derivatives were obtained in high purity.

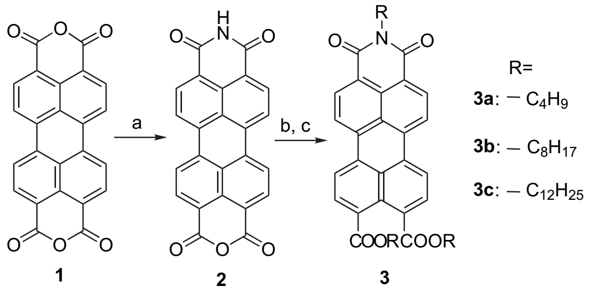

Scheme 1. Synthesis of the perylene monoimide diesters **3a**–**c**; (a) NH_3, H_2O, 90 °C, 2 h, 21%; (b) KOH, H_2O, 90 °C, 2 h; (c) TOAB, RBr, reflux, 1.5 h, 42% (**3a**), 58% (**3b**), 84% (**3c**).

Compounds **3a**–**c** are highly soluble in many common organic solvents, such as chloroform, dichloromethane, tetrahydrofuran, toluene, xylene, hexane, etc. The solubility of **3a**–**c** is several thousand times higher than that of the corresponding perylene diimides due to the attachment of the two flexible ester groups instead of one imide group onto one end of perylene core. The good solubility of **3a**–**c** will facilitate the fabrication of optoelectronic devices by solution-processing, such as spin-coating and cast-coating, which are extremely attractive for commercial applications in optoelectronic technologies due to the adaptability, simplicity, and low cost of manufacture.

2.2. Electrochemical properties

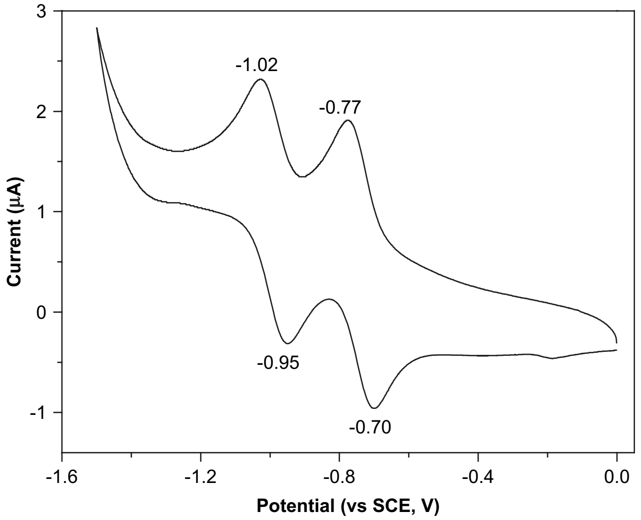

Figure 1. Cyclovoltammogram of **3c** tested in 0.1 M solution of Bu_4NClO_4 in dichloromethane with a scan rate of 50 mV/s.

The electrochemical properties of compounds **3a**–**c** were investigated by cyclic voltammetry in a 0.1 M solution of Bu_4NClO_4 in dichloromethane with a saturated calomel electrode (SCE) as the reference and Pt as the counter electrode. All compounds **3a**–**c** exhibit two reversible reduction waves, and Figure 1 shows the typical cyclovoltammogram of **3c**. The reduction potentials of **3a**–**c** are given in Table 1. Taking the first reduction potential and the potential of SCE versus the vacuum level (−4.74 eV) into account, the LUMO energy levels of **3a**–**c** can be calculated as $E_{LUMO}=-E_A=-4.74-E_{red}$,[24] and the results are listed in Table 1. The reduction potentials and E_{LUMO} of exemplified perylene diimide (**DPP**) and perylene tetraester (**PTE8**) are also listed in Table 1 for a clear comparison.[25,26] It is obvious that both the reduction potentials and E_{LUMO} of compounds **3a**–**c** show no obvious difference due to the energy node at the imide nitrogen and the ether oxygen.[14e] As expected, the E_{LUMO} of compounds **3a**–**c** is located between that of perylene diimide and that of perylene tetraester, which is the result of the different electron-withdrawing effects of the carbonyl in ester groups and imide groups due to their different coplanarity with perylene core. Compared with perylene tetraester, the lower E_{LUMO} of compounds **3a**–**c** would improve the electron-accepting property and thus favor the exciton dissociation at the donor/acceptor interface,[20] making **3a**–**c** potential n-type organic semiconductors for optoelectronic application.

2.3. X-ray diffraction

To investigate the influence of alkyl chain length on the structural ordering, X-ray diffraction (XRD) patterns of the sublimed **3a**–**c** thin films were recorded. As shown in Figure 2, all the XRD patterns of **3a**–**c** thin films show a peak at a small angle corresponding to a *d* spacing of 24.1, 27.6, and 22.6 Å, respectively, which is considered to be the distance between the adjacent π–π stacked

Table 1
Half-wave reduction potentials (in V vs SCE) and LUMO energy levels of compounds **3a**–**c**[a]

	DPP[b]	**3a**	**3b**	**3c**	**PTE8**[c]
E (**3**/**3**$^{-}$)	−0.51[b]	−0.77	−0.74	−0.74	−1.09[c]
E (**3**$^{-}$/**3**$^{2-}$)	−0.72[b]	−1.04	−1.00	−0.99	−1.39[c]
E_{LUMO} (eV)	−4.23[b]	−3.97	−4.00	−4.00	−3.65[c]

[a] Measured in 0.1 M solution of Bu_4NClO_4 in dichloromethane with a scan rate of 50 mV/s.

[b] **DPP**: *N*,*N*′-diphenyl perylene diimide. Cited from Ref. 25.

[c] **PTE8**: perylene tetraoctyl ester. Cited from Ref. 26.

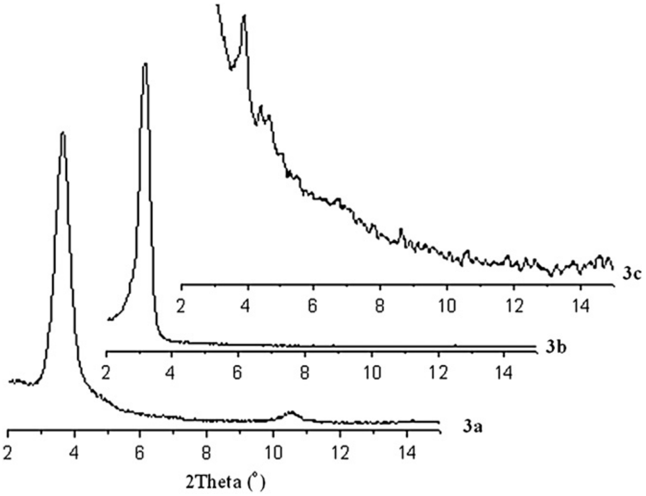

Figure 2. X-ray diffraction patterns of sublimed **3a–c** thin films on glass substrates.

perylene columns separated from each other by the alkyl chains.[27] Contrary to the expectation, **3c** has the shortest *d* spacing, indicating a significantly increased interdigitation of the long alkyl chains in **3c** and/or a large tilt angle of **3c** to the substrate. In addition, compound **3a** shows another peak at 10.46° with a *d* spacing of 8.45 Å, relating to the space of edge-to-edge arranged perylene cores,[27] which implies the formation of a more ordered film. However, the intensity of the diffraction peak of **3c** film is very weak, implying lower order as compared with **3a** and **3b** films. Therefore, it can be concluded that shortening of the alkyl chains results in an increase in film order. This effect was also found in perylene tetraester series.[28]

2.4. UV–vis spectroscopy

As shown in Figure 3A, the absorption spectra of compounds **3a–c** in chloroform are identical, which exhibit a fine structure with two peaks and one shoulder at 505, 475, and 446 nm, respectively. It is obvious that the alkyl chain length has no influence on the absorption spectra in solution, which is in agreement with earlier observations on perylene-based materials including perylene diimides and perylene tetraesters,[18,22] and is due to the nodes of the HOMO and LUMO orbitals at the imide nitrogen and the ether oxygen.[14e] In addition, the absorption peaks of compounds **3a–c** are located between those of perylene diimides (at 523, 487, and 454 nm) and those of perylene tetraesters (at 472, 444, and 417 nm),[22,28] which could be explained by their different π-electron delocalization owing to the different coplanarity with perylene core of the ester groups and imide groups.

Subsequently, the absorption spectra of compounds **3a–c** in evaporated films were recorded and were shown in Figure 3B. Unlike to the solution spectra, the absorption spectra of the evaporated **3a–c** films are obviously different. In the spectrum of **3a** film, four bands can be distinguished centered at about 549, 505, 481, and 458 nm. Compared with the solution spectrum, the spectrum of **3a** film shows an additional red-shifted absorption band at 549 nm. The absorption bands observed between 400 and 530 nm approximately coincide with those observed in the solution spectrum, but with vast differences in intensity compared with those in solution and strongly overlapping. It is considered that in this region the film shows at least one additional absorption band at around 480 nm as compared with the absorption maximum in solution.[27] Therefore, the film spectrum of **3a** shows two additional absorption bands, i.e., a blue-shifted band and a red-shifted band, upon going from (dilute) solution to film. On the contrary, the absorption spectra of **3b** and **3c** in evaporated films are similar, where the order of intensity for 0→0 (446 nm) and 0→2 (505 nm) vibronic transitions is thoroughly reversed compared with that in solution. In other words, the absorption maxima of **3b** and **3c** are blue-shifted, upon going from dilute solution to film.

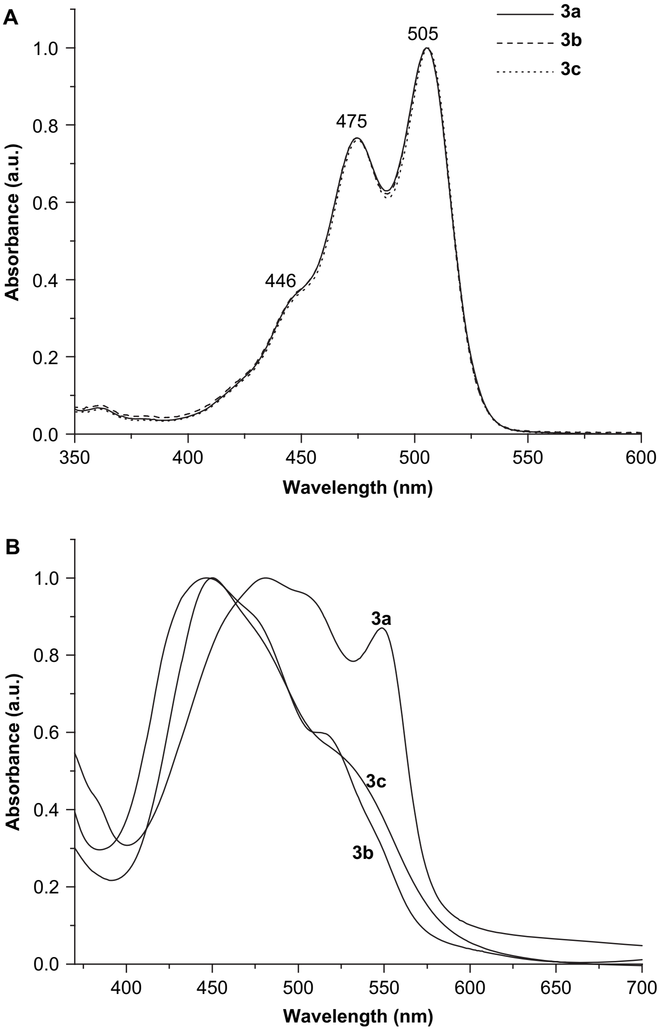

Figure 3. Normalized UV–vis absorption spectra of **3a–c** in chloroform (A) and in films vacuum-deposited on glass substrates at room temperature (B).

Spectral shifts observed upon aggregation of molecules are related to interchromophore distance and orientation and are often explained using the exciton coupling theory.[27,29] If the transition dipoles involved are oriented in a parallel fashion, a spectral shift to red or blue is expected depending on the angle between the center-to-center vector and the transition dipole moments of the adjacent chromophores. The critical angle is 54.7°. Above this critical value, a blue-shifted band is often observed and contrary is a red-shifted band appeared. If the transition dipoles involved are not parallel, a blue- and a red-shifted absorption bands are expected simultaneously, which may be the case with transition dipoles rotated with respect to each other while keeping the adjacent molecules parallel or the case with adjacent molecules oblique. So, the spectral shift of **3a** upon going from dilute solution to film can be explained in two ways: (i) more than one type of aggregates is present, and/or (ii) the transition dipole moments of adjacent molecules were not parallel. The above-mentioned XRD results of **3a** film have indicated that both head-to-tail and edge-to-edge configurations are present in **3a** aggregate, which will result in the appearance of red-shifted and blue-shifted bands, respectively. However, considering the inverse cube dependence of the exciton splitting on the intermolecular distance[30] and the large intermolecular distance in the two dimensions (2.41 and 0.845 nm, respectively), the spectral shift originated from the intermolecular interaction in the two directions might be ignored. Therefore, the spectral shift mostly originated from the π–π stacking of neighboring perylene cores in columnar stacks. Taking the parallel orientation of perylene skeletons in stacks of bay-unsubstituted perylene derivatives into account,[14e,31] we consider that the origin of the spectral shift of **3a** film should be the existence of a significant rotation between the transition dipole moments of adjacent **3a** molecules within one stack. This result is in agreement with earlier observations of a liquid crystalline perylene diimide.[27] On the contrary, aggregates as **3b** and **3c** films, which exhibit blue-shifted bands relative to the monomer absorption maxima, are conventionally referred to as H-aggregates and are thought of as untilted or slightly tilted ladder-like stacks.[32] It is noteworthy that there is a weak but detectable shoulder at about 535 nm in the spectra of **3b** and **3c**, which results from a nonvanishing transition probability between the ground and the lowest exciton state. This weak band may originate from vibronic coupling or a small rotational twist between adjacent chromophores.[32c,33] In addition, the spectrum of **3b** film is more blue-shifted compared with that of **3c** film, which may be due to a smaller difference of the van der Waals intermolecular energies in the ground and excited state (ΔD) resulting from the weak interdigitation of the alkyl chains.[29c,30,34]

It is well known that all highly photoactive materials show a substantial red-shifted absorption band coupled with substantial band broadening on aggregation.[32c] It is the stabilization of excitons in materials with substantial absorption broadening manifested as red shifts on aggregation that leads to an increase in exciton lifetime and thus allows more diffusion to the donor/acceptor interface in order to form separated holes and electrons. Therefore, **3a** with substantial band broadening is believed to be the most potential optoelectronic material in compounds **3a**–**c**. However, **3b** and **3c** might be potential electron transport materials due to the large overlap of π orbitals resulted from the slightly tilted ladder-like stacking configuration.

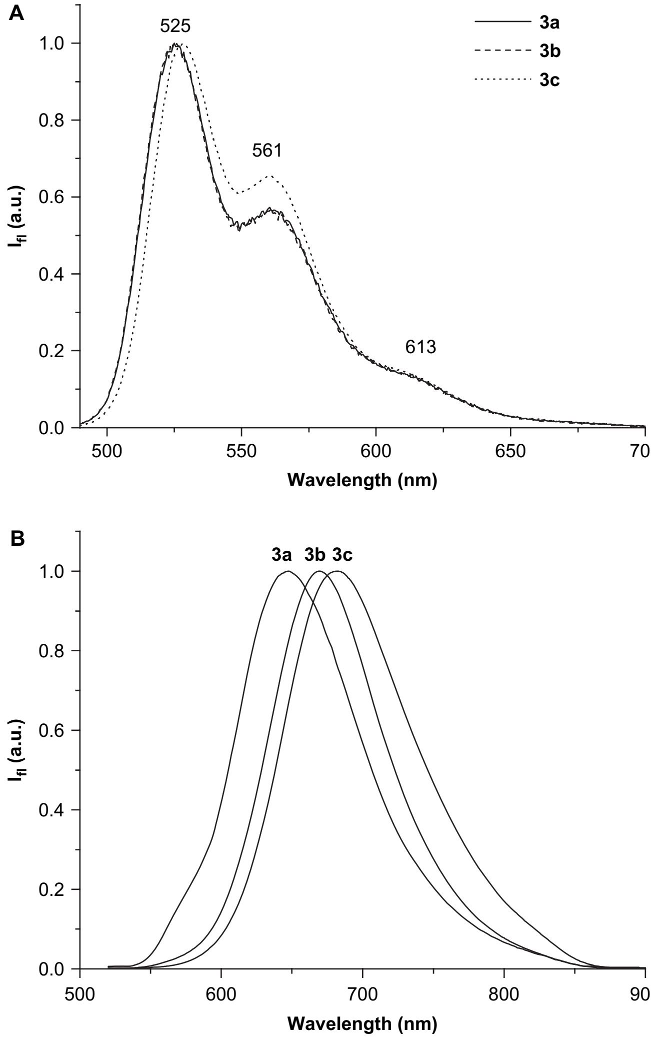

Figure 4. Normalized fluorescence spectra of compounds **3a**–**c** in chloroform (A) and in films vacuum-deposited on glass substrates at room temperature (B). The excited wavelength is 470 nm.

2.5. Fluorescence spectroscopy

The solutions of compounds **3a**–**c** in chloroform show a bright yellow fluorescence even under daylight, which is scarcely observed for the perylene-based fluorophores with the exception of the recently reported core-fluorinated perylene bisimides.[35] Figure 4A shows the fluorescence spectra of compounds **3a**–**c** in diluted chloroform solution, which exhibit a fine structure with two peaks and one shoulder at 525, 561, and 613 nm. The alkyl chain length has almost no influence on the fluorescence spectra in solutions. In addition, the fluorescence spectra of compounds **3a**–**c** fulfill the mirror image conditions to the absorption spectra (Fig. 3A) with Stokes shift of about 20 nm, which is larger than that of the corresponding perylene diimide ($\sim$14 nm)[22] due to the introduction of the flexible ester chains. Similar result was also observed for the corresponding perylene tetraesters.[28] Similarly, the fluorescence peaks of compounds **3a**–**c** are located between those of perylene tetraesters (at 493, 522, and 569 nm) and those of perylene diimides (at 536, 574, and 628 nm).[22,28] The emissive colors of perylene tetraesters, compounds **3a**–**c**, and perylene diimides in solution are bright green-yellow, bright yellow, and orange, respectively. Therefore, it is feasible to tune the emissive color of perylene-based fluorophores by attaching different kinds of substitutions on perylene core.

Figure 4B shows the fluorescence spectra of the evaporated **3a**–**c** films. It is found that one broad and featureless peak appears instead of the well-defined vibronic fine structure presented in the solution fluorescence spectra (Fig. 4A). The fluorescence maxima of films show remarkable red-shift ($>$100 nm) compared with those in solutions. Both the loss of fine structure and the large color shift are typical for fluorescence resulting from excimers (equal to excited dimers).[18] According to the above discussions on absorption spectra in films, **3a**–**c** films formed ground-state stable aggregates, so the excimers were formed when one monomer molecule in the stable aggregates was electronically excited due to absorption of a photon. Obviously, the emission maxima for **3a**–**c** films are greatly influenced by the length of the attached alkyl chains on perylene chromophores, and are 647, 670, and 682 nm for **3a**, **3b** and **3c**, respectively. It is noteworthy that a very weak shoulder appears at about 568 nm in addition to the band emission at 647 nm for **3a**; the shorter and longer wavelength emissions can be assigned to radiation from free and self-trapped excitons, respectively.[36] We consider that the main emission band for compounds **3a**–**c** results from the self-trapped excitons. Therefore, we conclude that the high different emission maxima of **3a**–**c** films originate from the different energy of emissive exciton traps, which is the result of their different order. With increasing the length of the alkyl chains, the film order decreases as verified by the above-mentioned XRD results, which means the existence of increased amount of grain boundaries and lower energy of emissive exciton traps, and thus the fluorescence maximum is red-shifted. Similar relationship between film order and fluorescence maxima was also observed in perylene films upon solvent vapor annealing.[32a]

3. Conclusions

Soluble perylene monoimide diesters were designed and synthesized for the first time, which exhibited essentially identical optical and electrochemical properties in solution located between those of perylene diimides and those of perylene tetraesters. While combining the absorption spectra of films with exciton coupling theory, it was deduced that the perylene moieties within a column were rotated in going from one layer to the other, and the rotation angle might dramatically decrease with increasing the alkyl chain length from 4 to 12 carbon atoms due to strong interdigitation between long alkyl chains. In addition, the emission maxima of films were red-shifted with the lengthening of alkyl chains, mainly due to the decreased order of films as proved by XRD measurements. In summary, by introducing imide and ester groups in one molecule, the resulting perylene monoimide diesters possess good solubility, acceptable electron-accepting ability, potential high charge carrier mobility and/or good photovoltaic property, which make these materials to be promising candidates in organic electronics applications. Our future interests are detailed characterization of their n-type semiconducting properties in application to organic field-effect transistors and solar cells.

4. Experimental

4.1. Materials

All solvents and reagents were obtained from commercial sources and used as received.

4.2. Equipments

FTIR spectra were measured on a Bruker Vector 22 FT-IR spectrometer. ^{1}H NMR spectra were obtained on a Bruker Avance DRX-300 NMR spectrometer. Elemental analyses data were determined on a Thermo Electron Flash EA-1112 element analysis apparatus. Cyclic voltammetry (CV) measurements were carried out on a CHI660A electrochemical workstation, tested in dichloromethane solutions containing 0.1 M supporting electrolyte of tetrabutylammonium perchlorate (Bu_4NClO_4) in a three electrode cell, where Pt disk, Pt wire, and saturated calomel electrode (SCE) were used as working electrode, counter electrode, and reference electrode, respectively. X-ray diffraction (XRD) measurements were performed on a Rigaku D/max diffractometer with Cu Kα radiation. The UV–vis absorption spectra and emission spectra were recorded on a Varian Cary 100 Bio spectrophotometer and on a Perkin Elmer LS55 fluorescence spectrophotometer, respectively.

4.3. Synthesis

*4.3.1. 3,4,9,10-Perylenetetracarboxylic-3,4-anhydride-9,10-imide (**2**)*

A mixture of 3,4,9,10-perylenetetracarboxylic dianhydride (**1**) (3.92 g, 10 mmol), water (100 ml), and aqueous ammonia solution (25%, 7.75 ml) was stirred at room temperature for 4 h. The mixture was then warmed to 90 °C and stirred at this temperature for 2 h. After the addition of a solution of 8 g potassium hydroxide in 200 mL water, the mixture was stirred for a further hour at 90 °C and the suspension was filtered to separate the insoluble diimide. Potassium chloride (30 g) was then added to the filtrate in order to precipitate out the potassium salt of **2**. The process was repeated several times. All the collected filter cakes, i.e., the potassium salt of **2**, were washed with 10% aqueous solution of potassium chloride until the filtrate was colorless in order to remove the more soluble salt of **1** completely (note: water should not be used). The filter cake was then dissolved in water at 90 °C and filtered using a frittered-glass funnel under vacuum to remove the insoluble byproduct thoroughly. After acidifying the filtrate with a minimum amount of 10% hydrochloric solution, the precipitate was collected, and washed with distilled water until the washings were neutral. The solid was then dried under vacuum, giving compound **2** with the yield of 21% (0.82 g). Compound **2** was further purified by train sublimation and used for characterization. IR (KBr): ν 1780, 1732 cm^{-1} (C=O in anhydride), 1695 cm^{-1} (C=O in imide). Elemental analysis (%) calcd for **2** ($C_{24}H_9NO_5$): C, 73.66; H, 2.32; N, 3.58. Found: C, 73.97; H, 2.23; N, 3.72.

*4.3.2. N-(n-Alkyl)-perylene-3,4-dicarboximide-9,10-di-(n-alkoxy-carbonyl) (**3**)*

A typical synthesis procedure for *N*-(*n*-alkyl)-perylene-3,4-dicarboximide-9,10-di-(*n*-alkoxy-carbonyl) (**3a**) was as follows: **2** (117 mg, 0.3 mmol) was converted to the dipotassium salt via stirring in aqueous potassium hydroxide solution (0.15 g in 150 mL water) at 90 °C. After filtration, the violet filtrate was acidified with 1 M hydrochloric solution until the pH value was 8–9. Then tetraoctylammonium bromide (TOAB) (60 mg) and 1-bromobutane (0.2 ml, ~1.8 mmol) was introduced, and the mixture was refluxed under vigorous stirring. After 1.5 h, the reactant solution became colorless and the reaction was ended. The product was collected by filtration and then was dissolved in chloroform. After filtration, the filtrate was collected and washed with 15% sodium chloride aqueous solution. The resulting chloroform solution was concentrated and precipitated by ethanol. After being washed with ethanol and deionized water, the product was dried under vacuum at 110 °C to give 72 mg (42% yield) **3a** as a red solid. FTIR (KBr): ν 2960, 2933, 2872, 1720, 1699, 1651, 1593, 1261, 1174, 746 cm^{-1}. ^{1}H NMR (300 MHz, $CDCl_3$), δ (ppm vs TMS)=1.00 (t, 9H, *J* 7.5), 1.43–1.51 (m, 6H), 1.75–1.80 (m, 6H), 4.21 (t, 2H, *J* 6.5), 4.35 (t, 4H, *J* 6.9), 8.08 (d, 2H, *J* 8.0), 8.42 (dd, 4H, *J* 8.0 and *J* 8.2), 8.58 (d, 2H, *J* 8.2). Elemental analysis (%) calcd for **3a** ($C_{36}H_{35}NO_6$): C, 74.85; H, 6.11; N, 2.42. Found: C, 74.79; H, 6.08; N, 2.49.

Compounds **3b** and **3c** were prepared in a similar way and their characterizations were shown below.

*4.3.2.1. Compound **3b**.* Yield 58%. FTIR (KBr): ν 2956, 2922, 2854, 1714, 1693, 1649, 1597, 1267, 1170, 748 cm^{-1}. ^{1}H NMR (300 MHz, $CDCl_3$), δ (ppm vs TMS)=0.85–0.90 (m, 9H), 1.20–1.54 (m, 30H), 1.76–1.84 (m, 6H), 4.19 (t, 2H, *J* 6.3), 4.33 (t, 4H, *J* 7.2), 8.10 (d, 2H, *J* 8.0), 8.42 (dd, 4H, *J* 8.0 and 8.0), 8.58 (d, 2H, *J* 8.0). Elemental analysis (%) calcd for **3b** ($C_{48}H_{59}NO_6$): C, 77.28; H, 7.97; N, 1.88. Found: C, 77.55; H, 8.04; N, 2.00.

*4.3.2.2. Compound **3c**.* Yield 84%. FTIR (KBr): ν 2956, 2918, 2849, 1725, 1698, 1654, 1598, 1257, 1163, 750 cm^{-1}. ^{1}H NMR (300 MHz, $CDCl_3$), δ (ppm vs TMS)=0.84–0.89 (m, 9H), 1.14–1.52 (m, 54H), 1.76–1.84 (m, 6H), 4.20 (t, 2H, *J* 6.6), 4.36 (t, 4H, *J* 7.2), 8.11 (d, 2H, *J* 8.0), 8.42 (dd, 4H, *J* 8.0 and 8.0), 8.59 (d, 2H, *J* 8.0). Elemental analysis (%) calcd for **3c** ($C_{60}H_{83}NO_6$): C, 78.82; H, 9.15; N, 1.53. Found: C, 78.96; H, 9.19; N 1.74.

Acknowledgements

This work was supported by National Natural Science Foundation of China (Grant No. 50433020, 50403022, 50520150165, 20774083) and by the Major State Basic Research Development Program (2007CB613402).

References and notes

1. (a) Newman, C. R.; Frisbie, C. D.; da Silva Filho, D. A.; Brédas, J.-L.; Ewbank, P. C.; Mann, K. R. *Chem. Mater.* **2004**, *16*, 4436–4451; (b) Ling, M. M.; Bao, Z. *Chem. Mater.* **2004**, *16*, 4824–4840; (c) Sirringhaus, H. *Adv. Mater.* **2005**, *17*, 2411–2425; (d) Horowitz, G. *Adv. Mater.* **1998**, *10*, 365–377; (e) Dimitrakopoulos, C. D.; Malenfant, P. R. L. *Adv. Mater.* **2002**, *14*, 99–117.
2. (a) Kulkarni, A. P.; Tonzola, C. J.; Babel, A.; Jenekhe, S. A. *Chem. Mater.* **2004**, *16*, 4556–4573; (b) Chen, C.-T. *Chem. Mater.* **2004**, *16*, 4389–4400; (c) Aziz, H.; Popovic, Z. D. *Chem. Mater.* **2004**, *16*, 4522–4532.
3. (a) Coakley, K. M.; McGehee, M. D. *Chem. Mater.* **2004**, *16*, 4533–4542; (b) Brabec, C. J.; Sariciftci, N. S.; Hummelen, J. C. *Adv. Funct. Mater.* **2001**, *11*, 15–26.
4. (a) James, D.; Scott, S. M.; Ali, Z.; O'Hare, W. T. *Microchim. Acta* **2005**, *149*, 1–17; (b) Adhikari, B.; Majumdar, S. *Prog. Polym. Sci.* **2004**, *29*, 699–766.
5. Yang, Y.; Ouyang, J.; Ma, L.; Tseng, R. J.-H.; Chu, C.-W. *Adv. Funct. Mater.* **2006**, *16*, 1001–1014 and references therein.
6. Sheats, J. R. *J. Mater. Res.* **2004**, *19*, 1974–1989.
7. Klauk, H.; Halik, M.; Zschieschang, U.; Schmid, G.; Radlik, W.; Weber, W. *J. Appl. Phys.* **2002**, *92*, 5259–5263.
8. (a) Bao, Z.; Dodabalapur, A.; Lovinger, A. J. *Appl. Phys. Lett.* **1996**, *69*, 4108–4110; (b) Sirringhaus, H.; Tessler, N.; Friend, R. H. *Science* **1998**, *280*, 1741–1744.
9. (a) Bao, Z.; Lovinger, A. J.; Dobabalapur, A. *Appl. Phys. Lett.* **1996**, *69*, 3066–3068; (b) Bao, Z.; Lovinger, A. J.; Dodabalapur, A. *Adv. Mater.* **1997**, *9*, 42–44.
10. (a) Chesterfield, R. J.; McKeen, J. C.; Newman, C. R.; Ewbank, P. C.; da Silva Filho, D. A.; Brédas, J.-L.; Miller, L. L.; Mann, K. R.; Frisbie, C. D. *J. Phys. Chem. B* **2004**, *108*, 19281–19292; (b) Malenfant, P. R. L.; Dimitrakopoulos, C. D.; Gelorme, J. D.; Kosbar, L. L.; Graham, T. O.; Curioni, A.; Andreoni, W. *Appl. Phys. Lett.* **2002**, *80*, 2517–2519; (c) Peumans, P.; Uchida, S.; Forrest, S. R. *Nature* **2003**, *425*, 158–162; (d) Shin, W. S.; Jeong, H.-H.; Kim, M.-K.; Jin, S.-H.; Kim, M.-R.; Lee, J.-K.; Leec, J. W.; Gal, Y.-S. *J. Mater. Chem.* **2006**, *16*, 384–390; (e) An, Z.; Yu, J.; Jones, S. C.; Barlow, S.; Yoo, S.; Domercq, B.; Prins, P.; Siebbeles, L. D. A.; Kippelen, B.; Marder, S. R. *Adv. Mater.* **2005**, *17*, 2580–2583; (f) Jones, B. A.; Ahrens, M. J.; Yoon, M.-H.; Facchetti, A.; Marks, T. J.; Wasielewski, M. R. *Angew. Chem., Int. Ed.* **2004**, *43*, 6363–6366.
11. Langhals, H. *Heterocycles* **1995**, *40*, 477–500 and references therein.
12. (a) Seybold, G.; Wagenblast, G. *Dyes Pigments* **1989**, *11*, 303–317; (b) Seybold, G.; Stange, A. D.E. Patent 3 545 004, 1987; *Chem. Abstr.* **1988**, *108*, 77134c.
13. (a) Oesterling, I.; Müllen, K. *J. Am. Chem. Soc.* **2007**, *129*, 4595–4605; (b) Cotlet, M.; Vosch, T.; Habuchi, S.; Weil, T.; Müllen, K.; Hofkens, J.; De Schryver, F. *J. Am. Chem. Soc.* **2005**, *127*, 9760–9768; (c) De Schryver, F. C.; Vosch, T.; Cotlet, M.; Van Der Auweraer, M.; Müllen, K.; Hofkens, J. *Acc. Chem. Res.* **2005**, *38*, 514–522; (d) Cotlet, M.; Masuo, S.; Luo, G.; Hofkens, J.; Van Der Auweraer, M.; Verhoeven, J.; Müllen, K.; Xie, X. S.; De Schryver, F. *Proc. Natl. Acad. Sci. U.S.A.* **2004**, *101*, 14343–14348.
14. (a) Kaiser, T. E.; Wang, H.; Stepanenko, V.; Würthner, F. *Angew. Chem., Int. Ed.* **2007**, *46*, 5541–5544; (b) Zhang, X.; Chen, Z.; Würthner, F. *J. Am. Chem. Soc.* **2007**, *129*, 4886–4887; (c) Sautter, A.; Kaletas, B. K.; Schmid, D. G.; Dobrawa, R.; Zimine, M.; Jung, G.; van Stokkum, I. H. M.; De Cola, L.; Williams, R. M.; Würthner, F. *J. Am. Chem. Soc.* **2005**, *127*, 6719–6729; (d) Dobrawa, R.; Lysetska, M.; Ballester, P.; Grüne, M.; Würthner, F. *Macromolecules* **2005**, *38*, 1315–1325; (e) Würthner, F. *Chem. Commun.* **2004**, 1564–1579.
15. (a) Tian, H.; Liu, P. H.; Zhu, W.; Gao, E.; Wu, D. J.; Cai, S. *J. Mater. Chem.* **2000**, *10*, 2708–2715; (b) Hua, J.; Meng, F.; Ding, F.; Li, F.; Tian, H. *J. Mater. Chem.* **2004**, *14*, 1849–1853; (c) Wang, S.; Shen, W.; Feng, Y.; Tian, H. *Chem. Commun.* **2006**, 1497–1499; (d) Pan, J.; Zhu, W.; Li, S.; Zeng, W.; Cao, Y.; Tian, H. *Polymer* **2005**, *46*, 7658–7669.
16. (a) Graaf, H.; Michaelis, W.; Schnurpfeilb, G.; Jaeger, N.; Schlettwein, D. *Org. Electron.* **2004**, *5*, 237–249; (b) Chen, Z.; Debije, M. G.; Debaerdemaeker, T.; Osswald, P.; Würthner, F. *ChemPhysChem* **2004**, *5*, 137–140.
17. Yamasaki, K.; Okada, O.; Inami, K.; Oka, K.; Kotani, M.; Yamada, H. *J. Phys. Chem. B* **1997**, *101*, 13–19.
18. Benning, S.; Kitzerow, H.-S. *Liq. Cryst.* **2000**, *27*, 901–906.
19. (a) Seguy, I.; Destruel, P.; Bock, H. *Synth. Met.* **2000**, *111–112*, 15–18; (b) Hassheider, T.; Benning, S. A.; Kitzerow, H.-S.; Achard, M.-F.; Bock, H. *Angew. Chem., Int. Ed.* **2001**, *40*, 2060–2063; (c) Seguy, I.; Jolinat, P.; Destruel, P.; Farenc, J.; Mamy, R.; Bock, H.; Ip, J.; Nguyen, T. P. *J. Appl. Phys.* **2001**, *89*, 5442–5448.
20. Oukachmiha, M.; Destruela, P.; Seguya, I.; Ablarta, G.; Jolinata, P.; Archambeaua, S.; Mabialaa, M.; Fouetb, S.; Bock, H. *Sol. Energy Mater. Sol. Cells* **2005**, *85*, 535–543.
21. Alibert-Fouet, S.; Dardel, S.; Bock, H.; Oukachmih, M.; Archambeau, S.; Seguy, I.; Jolinat, P.; Destruel, P. *ChemPhysChem* **2003**, *4*, 983–985.
22. Pasaogullari, N.; Icil, H.; Demuth, M. *Dyes Pigments* **2006**, *69*, 118–127.
23. Mo, X.; Chen, H. Z.; Shi, M. M.; Wang, M. *Chem. Phys. Lett.* **2006**, *417*, 457–460.
24. Ding, B.-d.; Zhang, J.-m.; Zhu, W.-q.; Zhen, X.-y.; Wu, Y.-z.; Jiang, X.-y.; Zhang, Z.-l.; Xu, S.-h *Chem. Res. Appl.* **2002**, *14*, 712–714.
25. Shi, M. M.; Chen, H. Z.; Sun, J. Z.; Ye, J.; Wang, M. *Chem. Commun.* **2003**, 1710–1711.
26. Mo, X.; Chen, H. Z.; Wang, Y.; Shi, M. M.; Wang, M. *J. Phys. Chem. B* **2005**, *109*, 7659–7663.
27. Struijk, C. W.; Sieval, A. B.; Dakhorst, J. E. J.; van Dijk, M.; Kimkes, P.; Koehorst, R. B. M.; Donker, H.; Schaafsma, T. J.; Picken, S. J.; van de Craats, A. M.; Warman, J. M.; Zuilhof, H.; Sudhőlter, E. J. R. *J. Am. Chem. Soc.* **2000**, *122*, 11057–11066.
28. Mo, X.; Shi, M. M.; Huang, J. C.; Wang, M.; Chen, H. Z. *Dyes Pigments* **2008**, *76*, 236–242.
29. (a) Kasha, M.; Rawls, H. R.; Ashraf El-Bayoumi, M. *Pure Appl. Chem.* **1965**, *11*, 371–392; (b) Würthner, F.; Thalacker, C.; Diele, S.; Tschierske, C. *Chem.—Eur. J.* **2001**, *7*, 2245–2253; (c) Lifshitz, E.; Kaplan, A.; Ehrenfreund, E.; Meissner, D. *J. Phys. Chem. B* **1998**, *102*, 967–973.
30. Graaf, H.; Schlettwein, D.; Jaeger, N. I. *Synth. Met.* **2000**, *109*, 151–155.
31. (a) Klebe, G.; Graser, F.; Hädicke, E.; Berndt, J. *Acta Crystallogr., Sect. B* **1989**, *45*, 69–77; (b) Zugenmaier, P.; Duff, J.; Bluhm, T. L. *Cryst. Res. Technol.* **2000**, *35*, 1095–1115.
32. (a) Gregg, B. A. *J. Phys. Chem.* **1996**, *100*, 852–859; (b) Furube, A.; Murai, M.; Tamaki, Y.; Watanabe, S.; Katoh, R. *J. Phys. Chem. A* **2006**, *110*, 6465–6471; (c) Kazmaier, P. M.; Hoffmann, R. *J. Am. Chem. Soc.* **1994**, *116*, 9684–9691.
33. Rösch, U.; Yao, S.; Wortmann, R.; Würthner, F. *Angew. Chem., Int. Ed.* **2006**, *45*, 7026–7030 and references therein.
34. Shi, M.-M.; Chen, H.-Z.; Shi, Y.-W.; Sun, J.-Z.; Wang, M. *J. Phys. Chem. B* **2004**, *108*, 5901–5904.
35. Würthner, F.; Osswald, P.; Schmidt, R.; Kaiser, T. E.; Mansikkama1ki, H.; Kolnemann, M. *Org. Lett.* **2006**, *8*, 3765–3768.
36. Tamai, N.; Porter, C. F.; Masuhara, H. *Chem. Phys. Lett.* **1993**, *211*, 364–370.